

Electronic Supplementary Information (ESI)

Structure diversities of ten entangled coordination polymers assembled from reactions of Co(II) or Ni(II) salts with 5-(pyridin-4-yl)isophthalic acid in the absence or presence of auxiliary N-donor ligands

Fei-Long Hu,^{ab} Mi Yan,^b Yun-Qiong Gu,^b Li-Gang Zhu,^b Sheng-Lan Yang,^b Han Wei,^b and Jian-Ping Lang^{*a}

^a College of Chemistry, Chemical Engineering and Materials Science, Soochow University, Suzhou 215123, Jiangsu, P. R. China.

^b College of Chemistry and Material, Yulin Normal University, Yulin 537000, P. R. China

Table of Contents

Fig. S1. (a) The 4-fold interpenetrating structure of 10 . (b) The pillar which formed by the short and/or long pillars.	S3
Fig. S2. PXRD patterns for 1-4 . (a) simulated (black) and single-phase polycrystalline sample (red) of 1 . (b) simulated (black) and single-phase polycrystalline sample (red) of 2 . (c) simulated (black) and single-phase polycrystalline sample (red) of 3 . (d) simulated (black) and single-phase polycrystalline sample (red) of 4	S3
Fig. S3. PXRD patterns for 5-8 . (a) simulated (black) and single-phase polycrystalline sample (red) of 5 . (b) simulated (black) and single-phase polycrystalline sample (red) of 6 . (c) simulated (black) and single-phase polycrystalline sample (red) of 7 . (d) simulated (black) and single-phase polycrystalline sample (red) of 8	S4
Fig. S4. PXRD patterns for 8-10 . (a) simulated (black) and single-phase polycrystalline sample (red) of 9 . (b) simulated (black) and single-phase polycrystalline sample (red) of 10	S4
Fig. S5. The TGA curves for compounds 1-3	S5
Fig. S6. The TGA curves for compounds 4-7	S5
Fig. S7. The TGA curves for compounds 8-10	S6
Magnetic properties	S7
Fig. S8. (a) $\chi_m T$ vs. T curve of 3 under 0.1 T applied field. (b) Field dependence of the magnetization of 3 at 2K. (c) Plot of χ^{-1} vs. T and the fit of Curie-Weiss law (red curve) of 3 . (d) Temperature dependence of magnetic susceptibilities in the forms of $\chi_m T$ at an applied field of 1 kOe and red solid line shows the best fit at 2–300 K.	S7

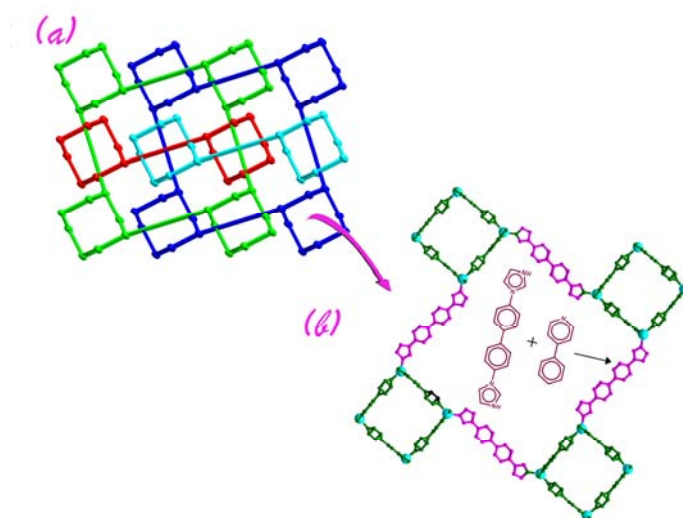


Fig. S1. (a) The 4-fold interpenetrating structure of **10**. (b) The pillar which formed by the short and/or long pillars.

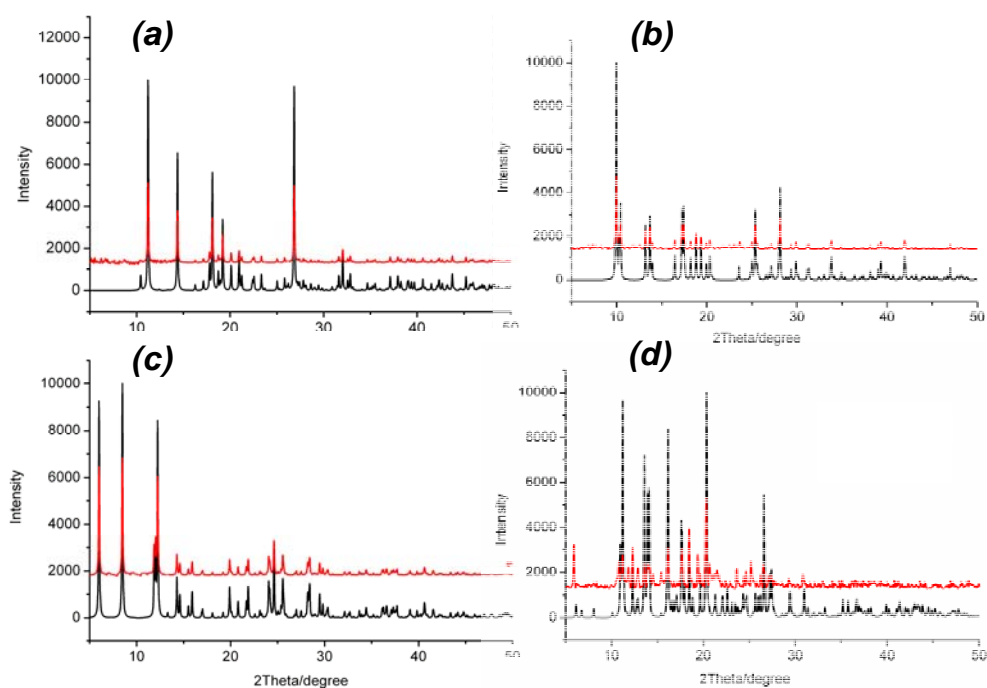


Fig. S2. PXRD patterns for **1-4**. (a) simulated (black) and single-phase polycrystalline sample (red) of **1**. (b) simulated (black) and single-phase polycrystalline sample (red) of **2**. (c) simulated (black) and single-phase polycrystalline sample (red) of **3**. (d) simulated (black) and single-phase polycrystalline sample (red) of **4**.

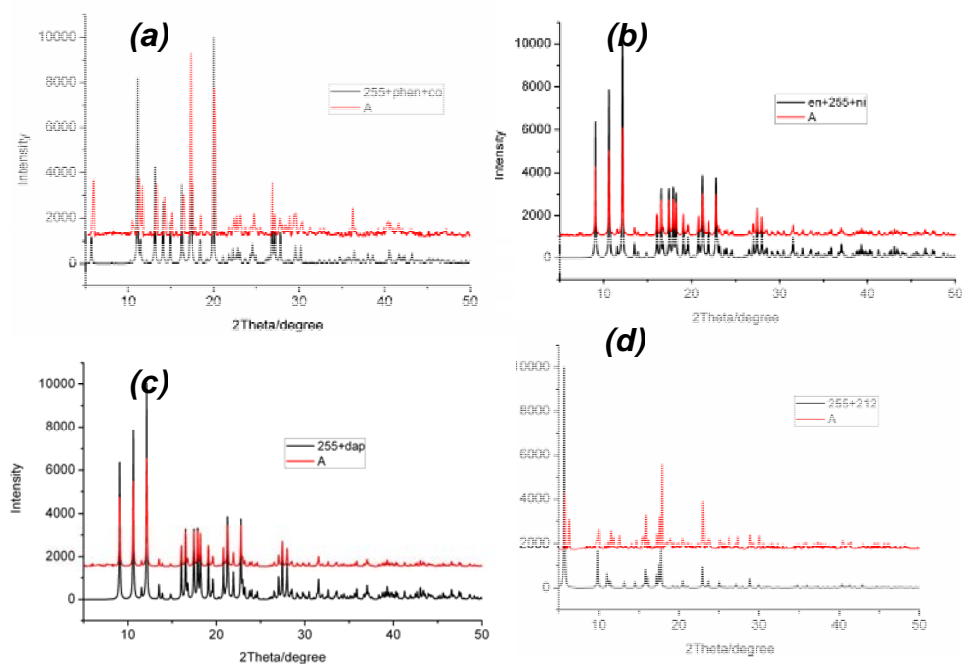


Fig. S3. PXRD patterns for **5-8**. (a) simulated (black) and single-phase polycrystalline sample (red) of **5**. (b) simulated (black) and single-phase polycrystalline sample (red) of **6**. (c) simulated (black) and single-phase polycrystalline sample (red) of **7**. (d) simulated (black) and single-phase polycrystalline sample (red) of **8**.

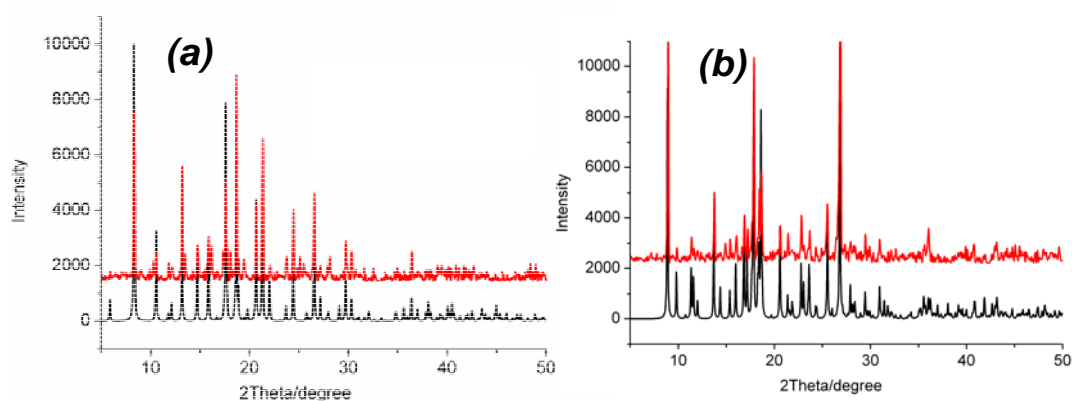


Fig. S4. PXRD patterns for **8-10**. (a) simulated (black) and single-phase polycrystalline sample (red) of **9**. (b) simulated (black) and single-phase polycrystalline sample (red) of **10**.

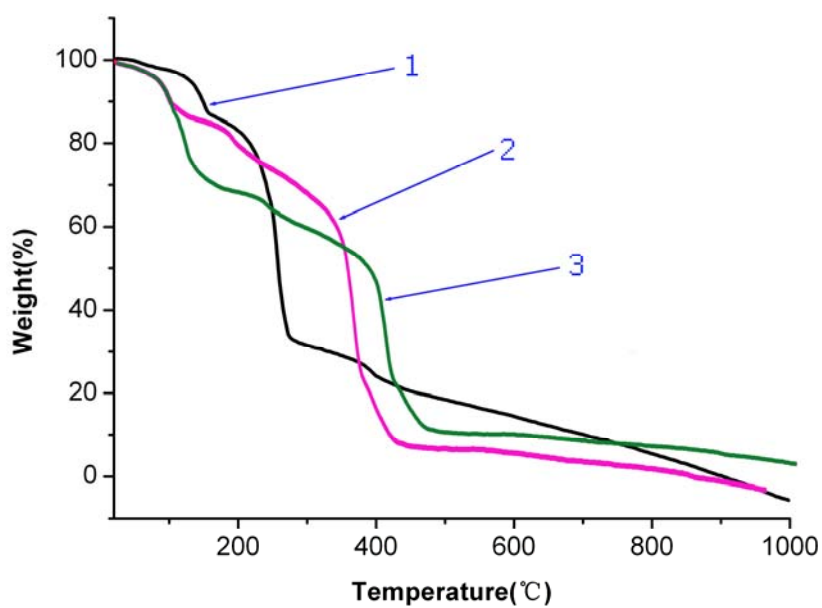


Fig. S5. The TGA curves for compounds 1-3.

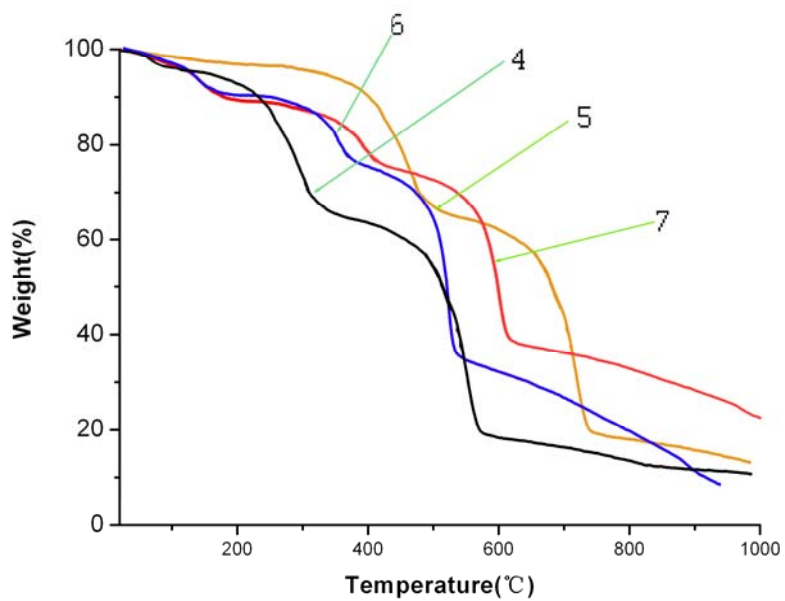


Fig. S6. The TGA curves for compounds 4-7.

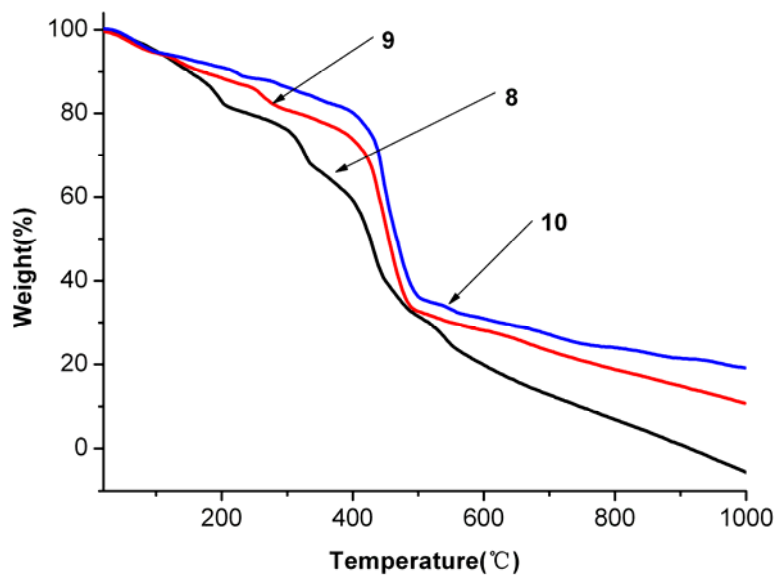


Fig. S7. The TGA curves for compounds **8-10**.

Magnetic properties

In order to further study the magnetic interactions in **3**, the noncritical-scaling theory with the following simple phenomenological Eqn (1) was used to fit experimental data from 300 to 2K.

$$\chi_m T = A \exp(-E_1/kT) + B \exp(-E_2/kT) \quad (1)$$

Here, A+B equals the high-temperature Curie constant for Co(II) cluster unit, and E_1 and E_2 represent the activation energies corresponding to the spin-orbit coupling and antiferromagnetic exchange interactions, respectively. The best fit of the experimental data gives $A + B = 9.1 \text{ cm}^3 \text{ K mol}^{-1}$, $E_1/k = 86.5 \text{ K}$, $E_2/k = 7.2 \text{ K}$. These values indicate that dominant antiferromagnetic interactions between Co(II) ions exist in **3**.

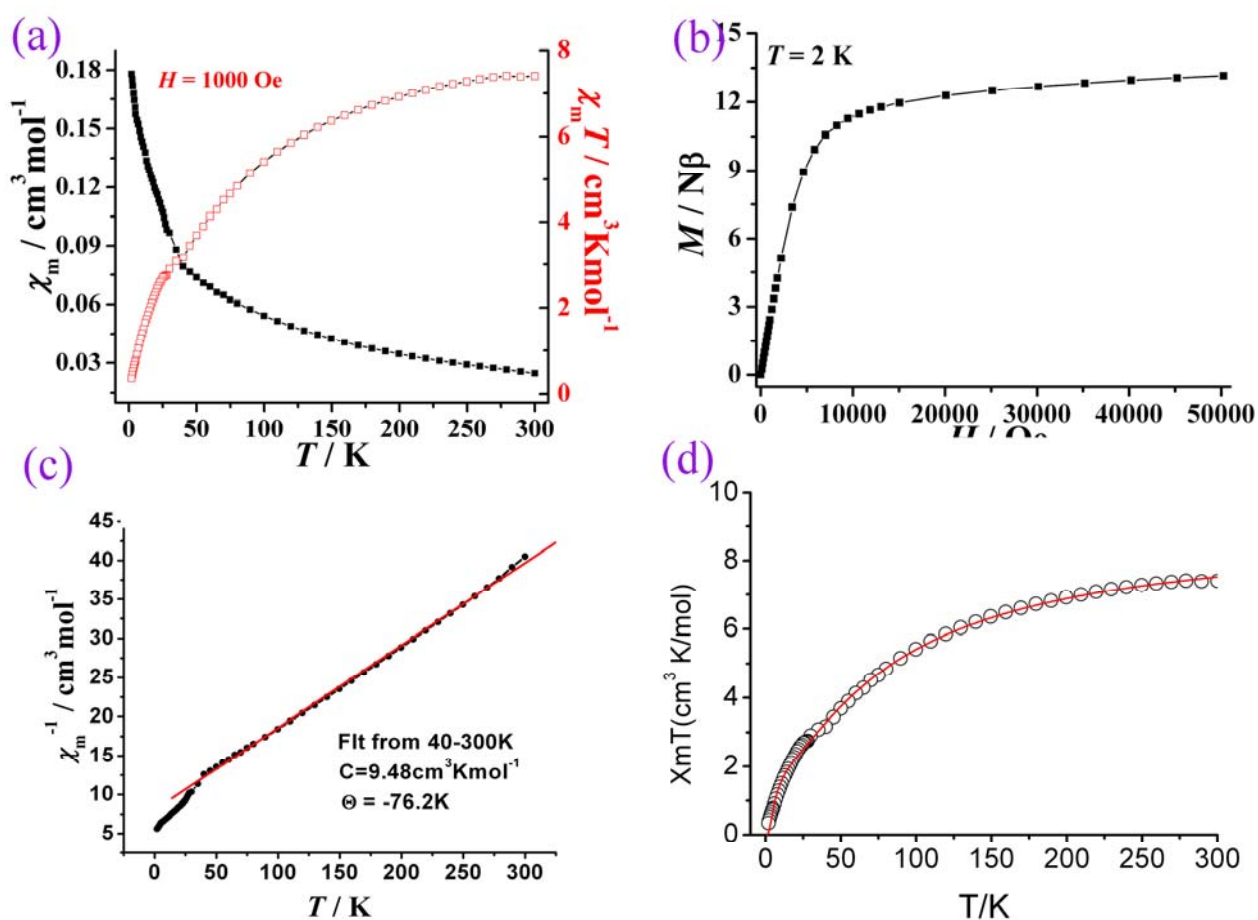


Fig. S8. (a) $\chi_m T$ vs. T curve of **3** under 0.1 T applied field. (b) Field dependence of the magnetization of **3** at 2K. (c) Plot of χ^{-1} vs. T and the fit of Curie-Weiss law (red curve) of **3**. (d) Temperature dependence of magnetic susceptibilities in the forms of $\chi_m T$ at an applied field of 1 kOe and red solid line shows the best fit at 2–300 K.